Supporting Information

Proteomic profiling of the oncogenic septin 9 reveals isoform-specific interactions in breast cancer cells

Louis Devlin[a,b], Joshua Okletey[a], George Perkins[b], Jonathan R. Bowen[a], Konstantinos Nakos[a], Cristina Montagna[c] and Elias T. Spiliotis[a*]

[a]Department of Biology, Drexel University, Philadelphia, PA 19095, USA

[b]Sanofi Pasteur, Swiftwater, PA 18370, USA

[c]Department of Radiology & Oncology, Rutgers Cancer Institute of New Jersey, New Brunswick, NJ 08901, USA

[*]Corresponding author:

Elias T. Spiliotis, Department of Biology, Drexel University, PISB 423, 3245 Chestnut St, Philadelphia, PA 19104, USA

E-mail: ets33@drexel.edu

Phone: 215-571-3552

Fax: 215-895-1273

Supporting Figures

Supporting Tables

Supporting Figures

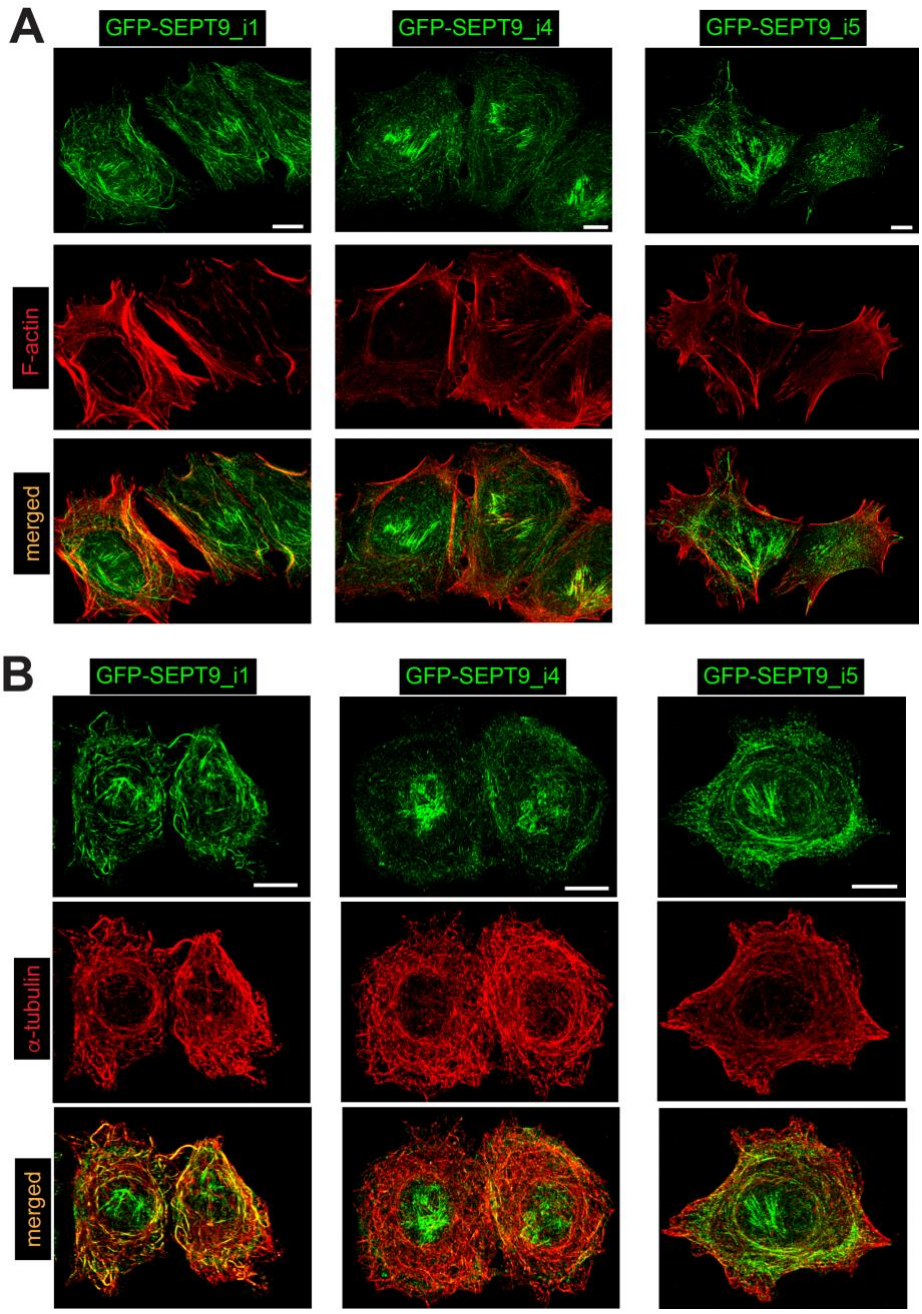

Figure S1. Localization of GFP-SEPT9 isoforms 1, 4 and 5 with respect to the actin and microtubule cytoskeleton. Images show maximal intensity projections of confocal microscopy sections taken from MCF-7 cells that express GFP-SEPT9_i1, GFP-SEPT9_i4 and GFP-

SEPT9-i5 after staining for actin filaments with phalloidin (A) and microtubules with an antibody against α-tubulin (B). Scale bars, 10 μM.

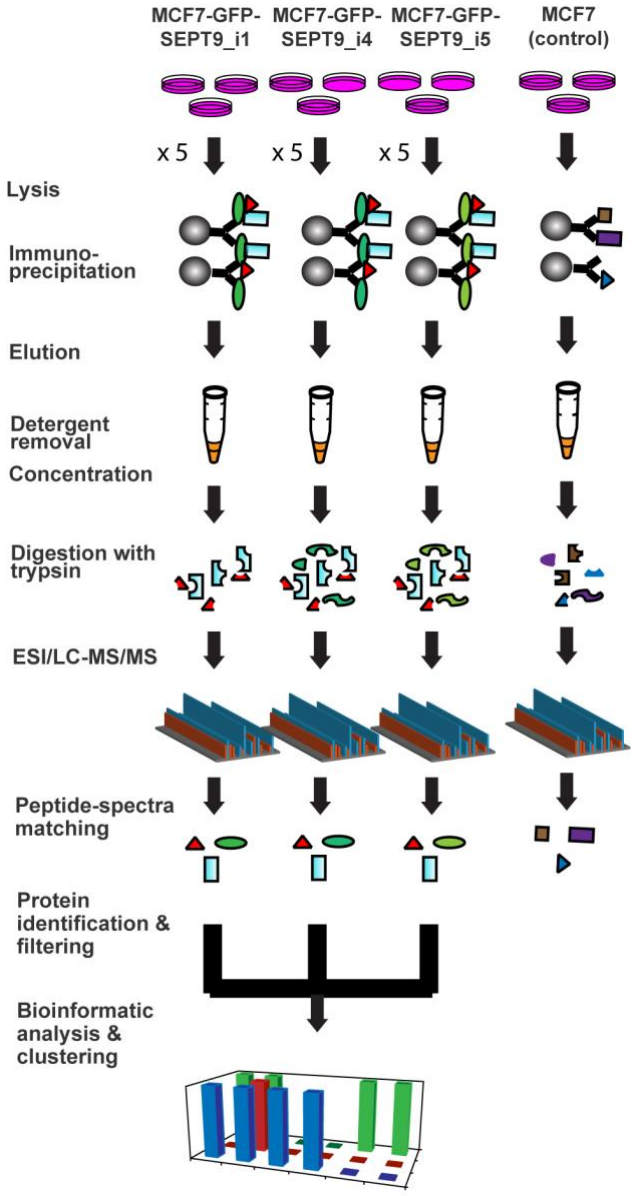

Figure S2. Workflow schematic of the proteomic screen. Each proteomic run was performed five independent times with each of the MCF-7 cell line expressing GFP-SEPT9_i1, GFP-SEPT9_i4 and GFP-SEPT9_i5 as well as non-transfected MCF-7 cells (negative control). In each independent experiment, three sub-confluent plates with MCF-7 cells were lysed and immunoprecipitations against GFP were performed in each of the three lysates. Eluants were

pooled, vacuum dried and digested with trypsin after detergent removal for injection into a liquid chromatography (LC) unit coupled to an electrospray ionization mass spectrometer (ESI-MS). Mass spectra were extracted and protein identities were derived by searches against the UniprotKB database. Data were filtered by applying quantitative thresholds to correct for non-specific interactions and contaminants, low-quality peptide-spectra and peptide-protein matches as well as low reproducibility. Data were analyzed for overlapping and unique binding partners, and non-septin binding partners were binned into subcellular organelle/structure and functional clusters.

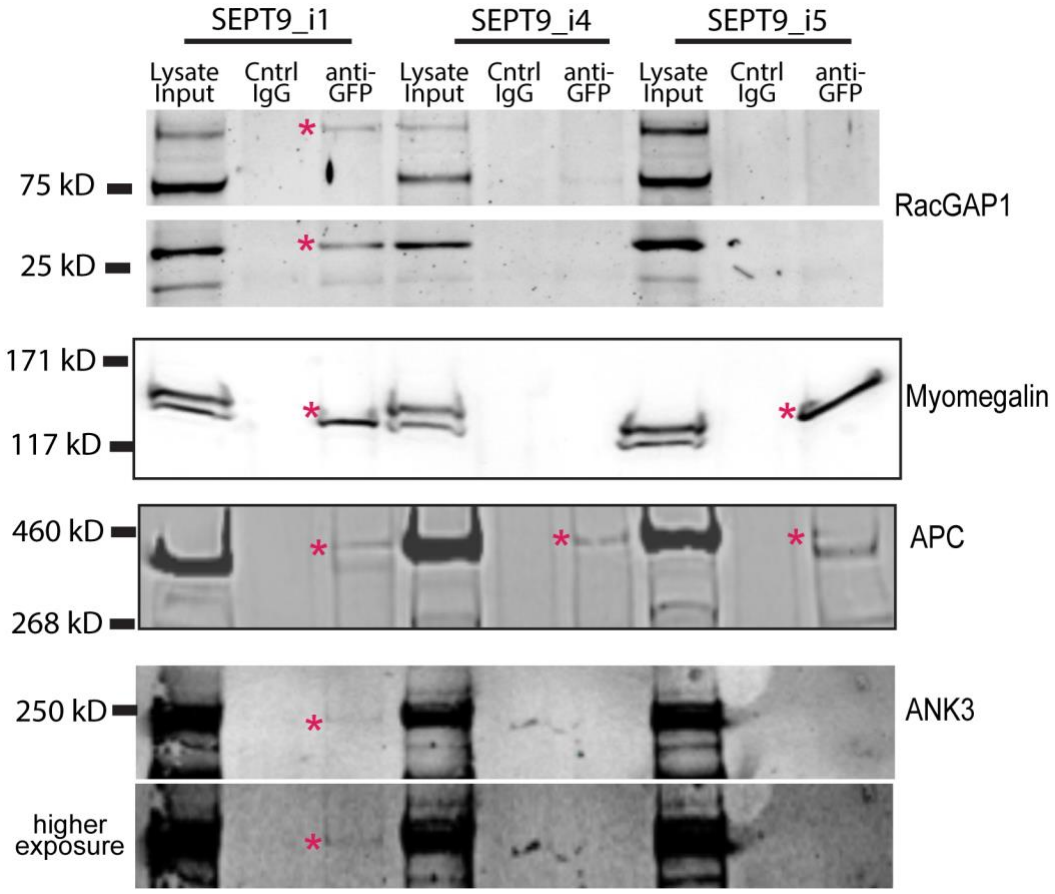

FIGURE S3. Validation of SEPT9 isoform hits RacGAP1, myomegalin, APC and ANK3 by western blotting. Lysates of MCF-7 cells expressing GFP-SEPT9_i1, GFP-SEPT9_i4 and GFP-SEPT9_i5 were treated with non-immune (control) and anti-GFP IgG antibodies. Whole

lysates and immunoprecipitates were western blotted for RacGAP1, myomegalin, APC and ANK3. The position of their corresponding protein bands in the anti-GFP immunoprecipitation lanes is denoted with a red asterisk.

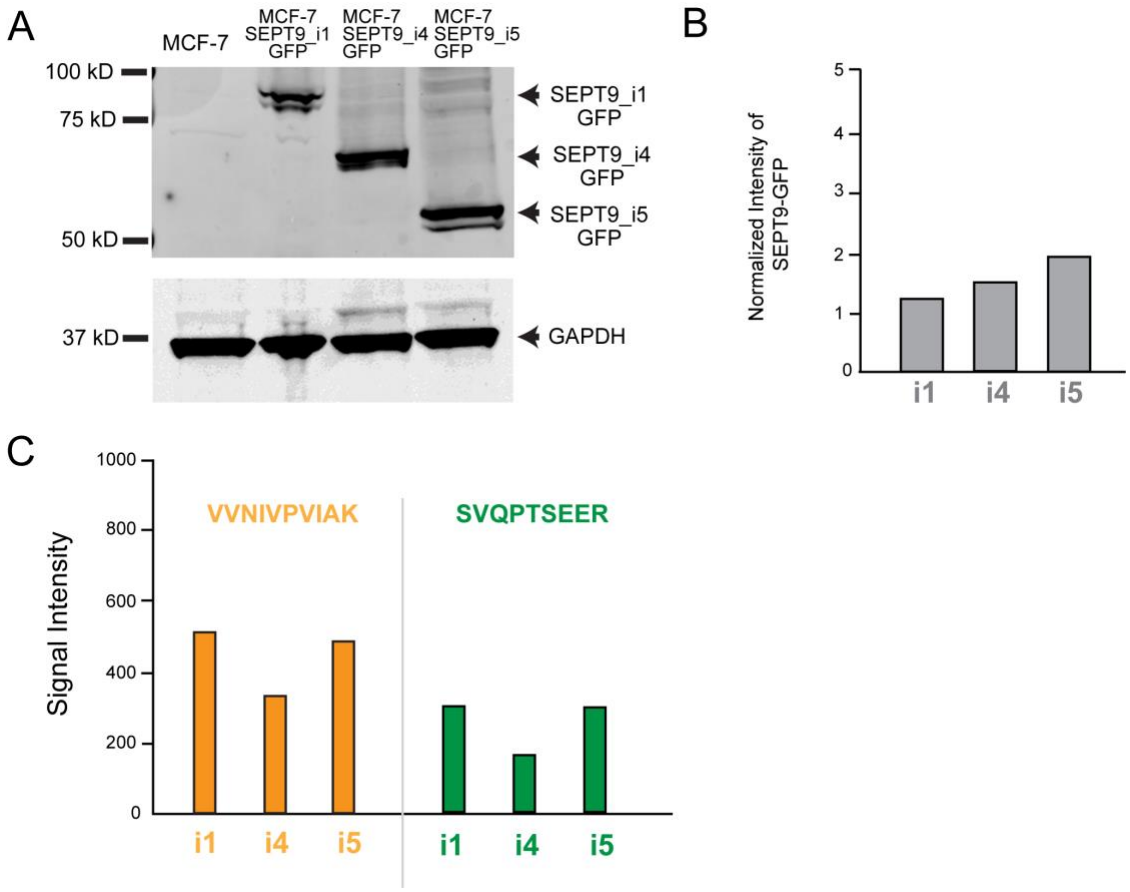

Figure S4. Relative abundance of SEPT9 isoform-specific peptides is independent of differences in GFP-SEPT9 expression levels. (A) GFP-tagged SEPT9 isoforms were immunoprecipitated with anti-GFP antibodies from MCF-7 lysates and western blotted with antibodies against GFP and GAPDH. (B) Bar graph shows the ratio of GFP to GAPDH band intensities. Quantifications were performed with a shorter exposure of the anti-GAPDH blot. (C) Bar graph shows the mass spec signal intensities of two peptides (VVNIVPVIAK and SVQPTSEER), which are shared among all SEPT9 isoforms. The signal intensities of shared peptides were nearly identical for isoforms 1 and 5, which exhibited the highest difference in expression levels.

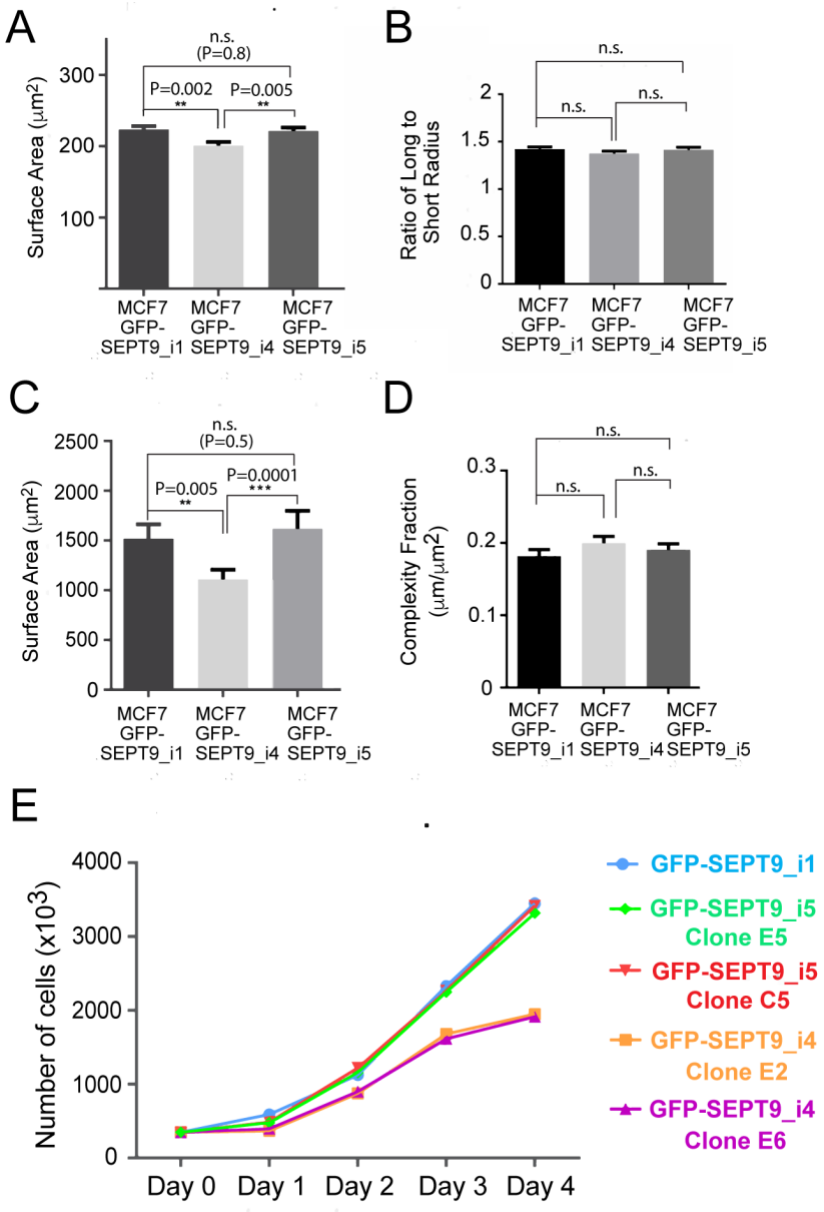

Figure S5. SEPT9 isoform 4 reduces cell and nuclear size, and proliferation. (A-B) The stable GFP-SEPT9-expressing MCF-7 cell lines, which were used for proteomic profiling, were fixed and stained with DAPI to label nuclei. Bar graphs show mean (± SEM) values of nuclear surface areas (A; n = 80 cells) and aspect ratios (B; ratio of long to short radius; n = 60 cells). (C-D). Bar graphs show mean (± SEM) cell size (C; n = 35) and complexity (ratio of perimeter length to surface area; n = 35), which were quantified in images of WGA-stained cells. (E) Plots show the growth of two different clones of stable MCF-7-GFP-SEPT9_i4 and -SEPT9-GFP-

SEPT9_i5 cell lines compared to MCF-7-GFP-SEPT9_i1. All cells were plated (day 0) in equal densities ($3.5x10^5$) and each point represents the average of three independent quantifications of cell numbers after 1, 2, 3 and 4 days of growth.

Supporting Tables

Table S1. List of proteins identified in all experimental runs. A comprehensive list of all protein identities (protein ID, accession numbers, description) and their corresponding probabilities of false discovery (-10lgP score), percent coverage, number and uniqueness of peptides, modifications and average mass. Each sheet shows proteins identified in individual experimental runs (Runs 1 to 5) from five independent immunoprecipitations with lysates of MCF-7 cells expressing SEPT9_i1, SEPT9_i4 or SEPT9_i5, and untransfected control cells. A cut-off score of -10lgP ≥ 15 (false discovery probability in peptide-to-spectrum and peptide-to-protein matching) was applied.

Table S2. Data for protein hits identified based on single peptides. Sheet entitled "summary" shows all protein hits across five independent immunoprecipitations denoted as runs 1, 2, 3, 4 and 5. Numbers under each run correspond to the number of peptides detected and number of total peptides across all five runs is shown under column G labeled as “total”. Accession number (protein identity), amino acid sequence, spectral match number and -10lgP score, retention times and uniqueness (Y, yes; N, no) are shown for each single peptide. Sheets entitled Run 1, Run 2, Run 3, Run 4 and Run 5 include annotated MS/MS spectra with ion match table including b and y ions, and an error map (including error tolerance) for each identified peptide. The peptide spectrum match (PSM) view shows peptide sequence, precursor mass, mass to charge ratio (m/z), retention time, mass error (ppm) and -10lgP values.

Table S3. CRAPome frequencies of detection and spectral counts for all non-septin hits. According the CRAPome database, frequency of detection (number of experiments found out of total experiments), CRAPome score, percentage of times detected, average spectral counts (Ave SC) and maximal spectral counts (Max SC) are tabulated for each non-septin interactor of GFP-SEPT9_i1 (sheet 1), GFP-SEPT9_i4 (sheet 2) and GFP-SEPT9_i5 (sheet 3) that was not

present in the negative control (untransfected MCF-7 cells) and met reproducibility, peptide-spectrum and peptide-protein threshold criteria. Shaded rows outline protein hits with CRAPome scores of >150, which were removed from the final list of protein hits.

Table S4. Spatial and functional categorization of all non-septin hits. Sheets 1 through 3 – All non-septin protein interactors of GFP-SEPT9_i1 (sheet 1), GFP-SEPT9_i4 (sheet 2) and GFP-SEPT9_i5 (sheet 3) are binned under subcellular organelles, structures and cytoskeletal systems; sheets 4 through 6 - all non-septin protein interactors of GFP-SEPT9_i1 (sheet 4), GFP-SEPT9_i4 (sheet 5) and GFP-SEPT9_i5 (sheet 6) are binned under subcellular organelles, structures and cytoskeletal systems.